Australian Earthquake Engineering Society
2021 Virtual Conference, Nov 25 – 26

Residual displacements of flexure-governed RC walls detailed with conventional steel and shape memory alloy rebars

Ryan D Hoult[1], João Pacheco de Almeida[1]

1. Institute of Mechanics, Materials and Civil Engineering, UCLouvain, Louvain-la-Neuve, Belgium.

Abstract

Recent seismic events have shown that permanent damage and deformations of buildings prevent the structure from being serviceable, imposing high costs associated with repairs or demolition. The yielding and inelasticity of the steel rebars in the boundary ends of modern-designed reinforced concrete walls are generally the source of residual displacements for reinforced concrete buildings. This paper investigates the residual displacement of reinforced concrete walls detailed with either conventional steel or shape memory alloys in the boundary ends of the wall. The force-displacement response of a large dataset of reinforced concrete flexurally-governed walls is analysed to derive the residual displacement as a function of in-plane displacement (or drift). The existing very few experimental results on reinforced concrete walls detailed with shape memory alloys are also examined. On average, walls detailed with conventional steel are found to attain residual displacement less than the permissible limit for drifts up to 1.5%. The shape memory alloy walls are generally shown to perform better, with an estimate of the permissible limit being reached at approximately 2.0% drift. However, some design deficiencies from two of three wall specimens detailed with shape memory alloys resulted in poor performance. Thus, more experimental testing is needed on reinforced concrete walls detailed with shape memory alloys to increase confidence in using these materials in practice.

Keywords: concrete, cores, plastic hinge, SMA, performance-based, design

1 Introduction

The philosophy for the modern design of reinforced concrete (RC) structures under earthquake actions intends to achieve predictable levels of performance in the event of specific seismic intensities. For a large earthquake intensity event, it is expected that modern RC buildings can sustain severe damage but prevent the collapse and safeguard against loss of life (Krawinkler & Miranda 2004). The performance objective matrix corresponding to this design philosophy is given in Figure 1a, which has been adapted from SEAOC (1995) and illustrates that it is acceptable for a building to be in a "life safe" or "near collapse" state for a rare or very rare earthquake event, respectively. While the primary performance level of no collapse for modern-designed RC structures can typically be achieved, the damage and permanent deformation of the structure can prevent the building from being serviceable and in some cases require demolition. Large post-earthquake residual displacements (i.e., the permanent relative deformation of a structure with respect to its foundation) impose very costly repairs and can require demolition and reconstruction of the entire building. For example, approximately 25% of all buildings in the central business district (CBD) of Christchurch were no longer vertical after the 2010-2011 earthquake sequence in New Zealand (Muir-Wood 2015). Many of these building tilts were in such excess that they were required to be demolished after being declared "uneconomic to repair". An extreme example of this is the Grand Chancellor Hotel, one of the tallest buildings in Christchurch, which had a permanent, distinct twist and lean after the earthquake, with residual displacements around 200-400 mm (Kam et al. 2011). The general public is typically overwhelmed by the end result (e.g., the extent of damage, cordoning off of the CBD, disruption to services) (Goldsworthy 2012). As such, a revised performance matrix was proposed by Buchanan et al. (2011) in Figure 1b, which shows that under a rare or very rare earthquake event a building should be designed to remain operational or fully operational. To achieve these targets, engineers would not only have to design for larger seismic loads but also implement better structural technologies (Goldsworthy 2012).

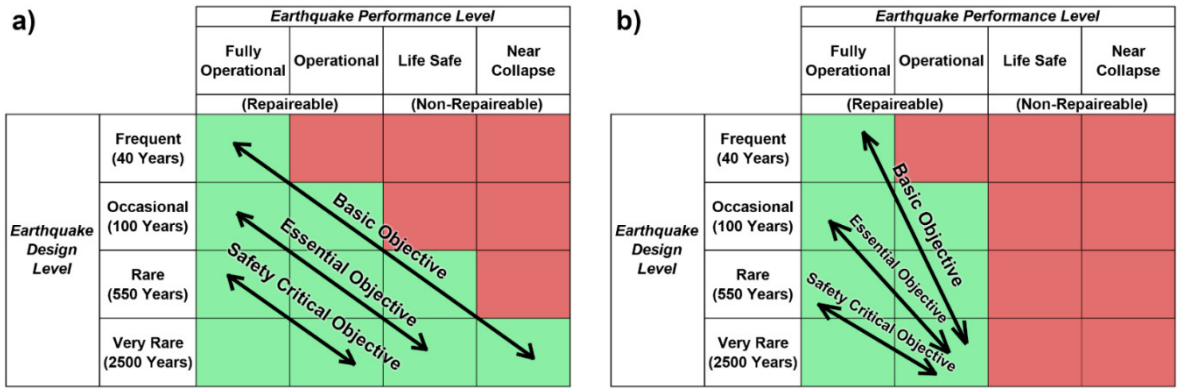

Figure 1. (a) Current Performance Objective Matrix adapted from SEAOC (1995) (b) proposed Performance Objective Matrix adapted from Buchanan et al. (2011)

Structural walls are typically used as the primary lateral load resisting system in RC buildings to forces and displacements generated from wind and earthquakes (Dashti et al. 2020). Modern seismic design standards (e.g., AS 3600:2018; NZ 3101:2006; CEN 2004; ACI 318-19) promote flexural ductility and intend to prevent brittle failure modes. A typical feature of modern RC walls designed for large moments are "boundary elements" (i.e., regions located at wall ends, Figure 2) detailed with additional longitudinal reinforcement (Sritharan et al. 2014). In earthquake events, these boundary regions of the wall will be subjected to the largest tensile strains (Rosso et al. 2020), and thus the yielding and inelasticity of the steel rebars in the boundary ends of the wall are typically the source of residual displacements for RC buildings.

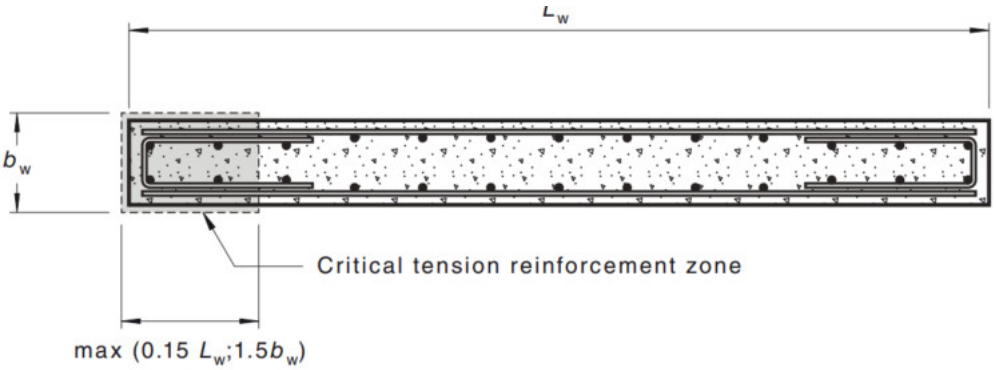

Figure 2. Location of the boundary region of a planar RC wall section from AS 3600:2018 (herein without additional longitudinal reinforcement)

This research investigates the residual displacement of reinforced concrete walls detailed with conventional steel and shape memory alloys (SMAs) in the boundary ends of the wall. A large database of tested RC wall specimens and the associated reverse-cyclic force-displacement response is used to determine the residual displacement of these walls as a function of drift. Furthermore, a small number of experimental wall specimens detailed with SMA bars are equally used to investigate the residual displacement.

In the next section, engineering demand parameters that are typically used to estimate the seismic performance of RC buildings are presented. Importantly, a permissible limit for the residual displacement of RC walls is also presented, which will be used in this research.

2 Limitations on drifts and residual displacements

One relevant engineering demand parameter typically used to evaluate the seismic performance of a building is the inter-story drift. The inter-story drift is the ratio of the lateral displacement between two consecutive floors to the floor height, whereas the average drift is the ratio of top building displacement to building height. Performance objectives (or levels), such as those in Figure 1, can be associated to the level of damage of the structure, which can then be related to the level of drifts experienced by the structure (Ghobarah 2001). Adopted from Ghobarah (2001) and based on performance levels from SEAOC (1995), Table 1 provides estimated inter-story drift levels corresponding to damage states and warranted performance objectives. However, as argued in McCormick et al. (2008), the economic losses that are associated with partially collapsed structures suggests that residual displacements of buildings also need to be considered as a limit state within the performance-based seismic design framework. Based on building functionality, construction tolerance levels, and structural safety, McCormick et al. (2008) recommend a permissible residual drift level of 0.005 rad. Thus, a residual drift value of 0.005 rad (or 0.5%) is adopted for this study corresponding with an operational performance level.

Table 1 Performance objectives corresponding to damage states and inter-story drift limits (adopted from Ghobarah, 2001)

Performance Objective	Damage State	Inter-story Drift
Fully Operational	No Damage	<0.2%
Operational	Repairable	<0.5%
Life Safe	Irreparable	<1.5%
Near Collapse	Severe	<2.5%
Collapse	-	>2.5%

3 Residual displacement of conventional RC walls

There has been a considerable effort by the engineering research community to conduct a large number of experimental tests on rectangular RC walls detailed with conventional steel and with a range of design parameters, consistent with current industry practice internationally. The SERIES RC wall database (Perus et al. 2014) and the NEEShub RC wall database (Lu et al. 2010) were used to compile as many force-displacement hysteresis of rectangular RC walls as possible for the purposes of determining the residual displacement (Δ_{res}) as a function of in-plane drift (δ). The walls selected from the databases complied to the following criteria: (i) shear-span-ratio (e.g., $M/VL_w = H_e/L_w$) equal to or greater than 2.0 for flexurally governed walls, (ii) rectangular cross-section, where non-planar walls are out of the scope of this research investigation, and (iii) subjected to a reverse-cyclic loading protocol. To complement the compiled walls from the two databases noted above, more recent wall tests with available datasets were also used. In total, 76 RC wall specimens detailed with conventional steel were used to investigate the Δ_{res} as a function of δ. The full list of wall specimens, corresponding references, and design parameters can be found online (see Section 8 – Data Availability). The range of design values for some of the wall parameters are given in Table 2, where a minimum, mean, and maximum are indicated. It should be noted that in Table 2, t_w is the wall thickness, L_w is the wall length, L_v is the shear span ($=M/V$), ALR is the axial load ratio, ρ_{lb} is the longitudinal reinforcement ratio in the boundary end regions of the wall, and ρ_{lw} is the longitudinal reinforcement ratio in the web of the wall.

Table 2 Range of design values for some of the wall parameters used by the experimental test specimens

	t_w (mm)	L_w (mm)	L_v (mm)	ALR (%)	ρ_{lb} (%)	ρ_{lw} (%)
Minimum	50.00	400.00	1050.00	0.00	0.24	0.15
Mean	121.43	1160.70	3061.20	18.21	1.65	1.01
Maximum	200.00	3048.00	10000.00	86.00	3.67	3.67

The experimental force-displacement relationship from all 76 walls (Table A1, see Section 9) were used to derive a total of 2241 data points of the residual displacement (Δ_{res}) and the corresponding in-plane drift (δ). Figure 3a illustrates how this data is compiled, where the last cycle of the force-displacement hysteresis from specimen TW1 (Almeida et al. 2017) is used for this example. Figure 3a shows that the in-plane drift (δ) is firstly recorded, corresponding to the maximum force (F_{max}) experienced in the cycle, after which the Δ_{res} can be determined (i.e., the displacement at zero force upon returning to the initial position of the wall). Figure 3b plots these data points, where Δ_{res} is normalised to the wall specimen height (h_s) (and is given in mrad). The in-plane drift indicated in Figure 3b is the maximum (in absolute value) achieved by the wall prior to the residual displacement observed on reverse loading (Figure 3a). A second order polynomial line-of-best-fit ("LOBF") is superimposed in Figure 3b. The above discussed permissible limit of 0.005 rad (or 5 mrad), used in this research to indicate onset of a non-serviceable building is also indicated in Figure 3b. These experimental results of RC walls detailed with conventional steel indicate that an average drift of approximately 1.5% can be attained prior to reaching this permissible limit imposed on the residual displacements. Equation 1 is derived from the LOBF, which can estimate the normalised residual displacement (Δ_{res} / h_s) as a function of the in-plane drift (δ, in percent) imposed on the wall.

$$\Delta_{res}/h_s = 0.0022\delta^2 \quad (1)$$

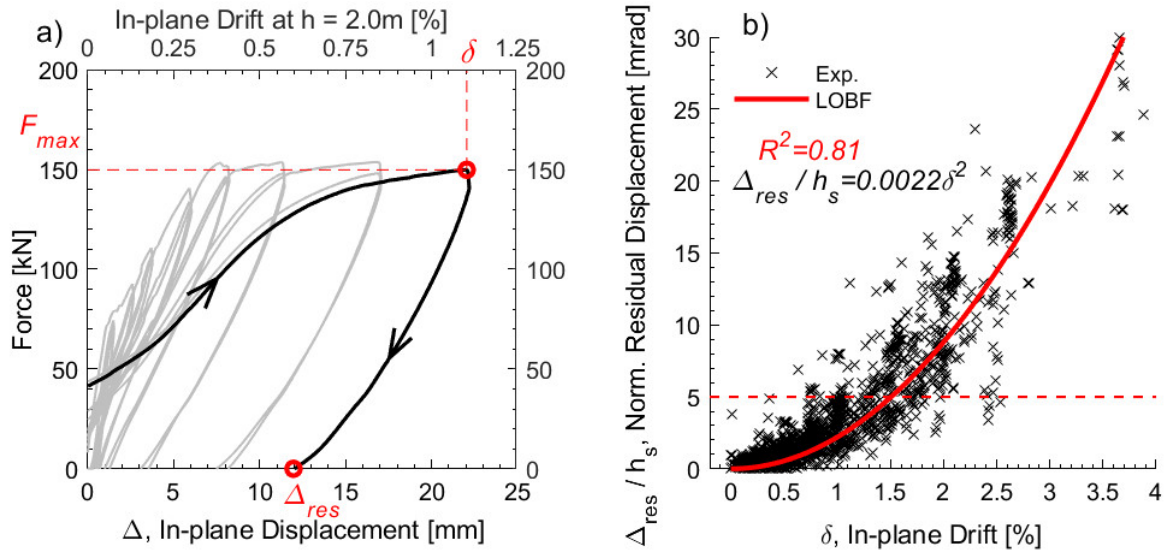

Figure 3 (a) calculation of residual displacement (Δres) using the experimental force-displacement hysteresis (b) normalised ("Norm.") residual displacement (in mrad) as a function of in-plane drift from the dataset of experimental RC walls with conventional steel

4 Residual displacement of RC walls with shape memory alloys

Shape memory alloy (SMA) bars have recently attracted some interest from researchers and structural engineers primarily due to their ability to (i) recover displacements upon removal of stress, (ii) dissipate energy through hysteretic damping, and (iii) provide strength and displacement capacities comparable to conventional deformed reinforcement (Jani et al., 2014). For example, the stress-strain relationship of a typical NiTi SMA rebar, adopted from Almeida *et al*. (202), is illustrated in Figure 4a, which is compared to the typical behaviour observed for a ductile reinforcing bar. Thus, it is for these reasons that SMA bars have the potential to be used as reinforcement in wall boundary ends, aiming at reducing residual displacements and ultimately decrease societal and economic impacts after seismic events. More detailed information on the phase transformations responsible for the SMA bars behaviour can be found in Graesser and Cozzarelli (1991). As previously mentioned, RC walls subjected to bending will undergo its largest tensile strains in the boundary ends of the wall. Thus, it has been argued that the placement of SMA rebars can be restricted to the boundary end regions of the wall (Almeida et al. 2020), significantly reducing the quantity of SMA bars required, as well as their associated costs.

To the knowledge of the authors, there have only been three experimental research investigations focusing on RC walls detailed with SMA bars. Two RC-SMA walls were tested with almost identical detailing for a limiting shear span of 2.2 and no applied axial load (Abdulridha & Palermo 2017; Kian & Cruz-Noguez 2018). More recently, Almeida et al. (2020) tested a single RC-SMA wall with a larger shear span of 3.6. However, budget constraints resulted in a SMA bar length of just 270 mm, limiting the yielding length and restricting the displacement capacity of the wall. For the sake of brevity, the readers are directed to the corresponding journal papers for more information on the specifics of these wall specimens. The list of these wall specimens, corresponding references, and some of the salient design parameters can be found online (see Section 8 – Data Availability).

The experimental force-displacement relationship from the 3 walls (Table A2, see Section 9) were used to derive a total of 132 data points of Δ_{res} and the corresponding δ. This was compiled using the same procedure illustrated in the previous section (Figure 3a). The compiled data for the RC-SMA walls is plotted in Figure 4b, where Δ_{res} is normalised to the shear span (L_v) (and is given in mrad). A second order polynomial line-of-best-fit ("LOBF") (Equation 2) is superimposed in Figure 4b. Consistent with the previous section, the same

permissible limit of 0.005 rad (or 5 mrad) for a non-serviceable building is also indicated in Figure 4b. While the dataset used is limited, these experimental results of RC-SMA walls indicate a slightly better performance, on average, in comparison to the trends presented in Figure 3b for RC walls detailed with conventional steel. According to the data in Figure 4b, an average drift of approximately 2.0 % can be attained prior to reaching this permissible limit imposed on the residual displacements. Building standards or codes generally limit the maximum inter-story drifts in buildings from 2.0 to 2.5% (ASCE, 2010; NRCC, 2010); the Australian Standards conservatively limits the drift to 1.5% (Standards Australia 2007).

$$\Delta_{res}/h_s = 0.0012\delta^2 \quad (2)$$

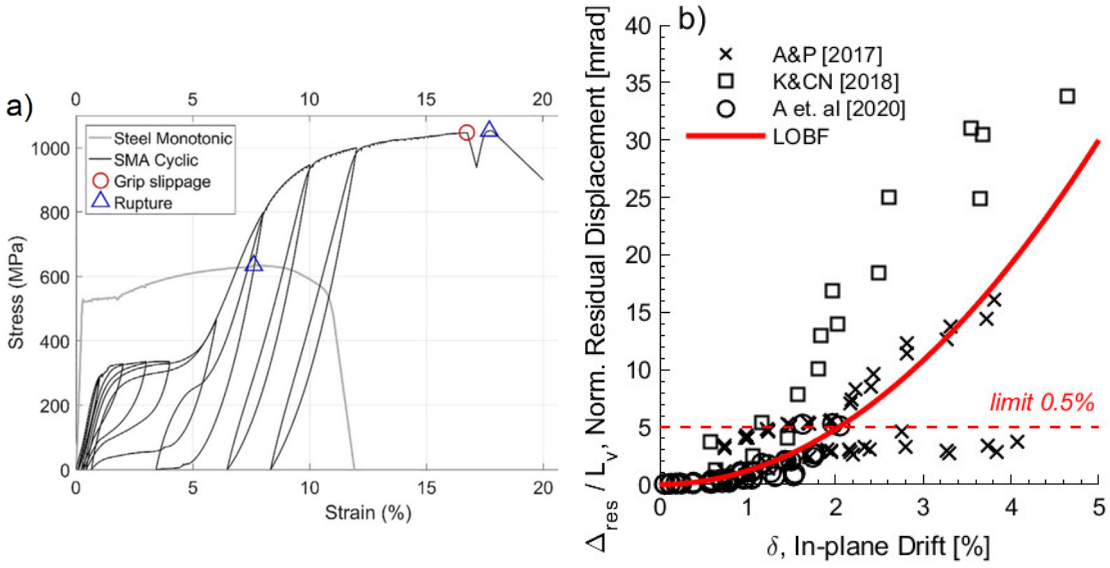

Figure 4 (a) Stress-strain relationship of a NiTi SMA rebar in comparison to reinforcing steel bar from Almeida et al. (2020) (b) Normalised ("Norm.") residual displacement (in mrad) as a function of in-plane drift from the limited dataset of experimental RC-SMA walls

Some of the poor performance observed in Figure 4b, indicated by the residual displacement datapoints greater than the limit of 5 mrad, can be attributed to the low amount of longitudinal reinforcement used in the web of the wall. For example, wall specimen W2-NR from Abdulridha & Palermo (2017) was found to have some premature softening of the wall in one direction of loading and early rupturing of the steel rebars in the web. Similarly, the wall specimen from Kian & Cruz-Noguez (2018) also experienced rupturing of the steel reinforcement in the web, whereas the SMA rebars in the boundary ends remained intact at the end of the test. In these cases, the source of the residual displacement appeared to be due to a concentration of strain in the low amount of steel in the web, which caused these bars to yield prematurely and deform permanently with each cycle. This type of behaviour is not too dissimilar to what was observed after the 2011 Christchurch earthquake, where walls with a light amount of longitudinal steel reinforcement in the web and greater concentrations in the boundary ends were found to perform poorly, with crushing of the wall occurring in the web region (Rosso et al. 2014). This type of damage pattern was also observed experimentally in wall tests that included a number of specimens with lumped longitudinal reinforcement in the boundary ends (Brueggen et al. 2017). Furthermore, a low amount of steel in the web has been found to cause unwarranted behaviour of shear sliding along a large-open crack (Aaleti et al. 2013), similar to what has been observed for these RC-SMA wall specimens. Thus, it is likely that RC-SMA walls can achieve much lower residual displacements (as a function of drift) from that indicated in Figure 4b if the appropriate measures of reinforcement detailing are provided.

5 Future Research

The results from this research investigation indicate that shape memory alloys could be used as a substitute material for conventional steel in the boundary ends of RC walls to reduce residual displacements. This type of structural detailing has the potential to provide the strength and displacement capacity requirements while limiting its performance range to be operational in the event of a rare or very rare earthquake event, which would significantly reduce societal and economic impacts. While these results are promising, further experimental research on RC walls detailed with SMA bars is required to confirm this performance, particularly with regards to the potential of other failure modes occurring that were not considered here (e.g., out-of-plane buckling and instability).

6 Conclusions

While engineers are typically satisfied with the “Life Safe” and “Near Collapse” performance of modern RC buildings observed in recent large earthquake events, the public can be overwhelmed by the indirect effects caused by the extent of residual displacements and damage to buildings, interruptions to services, and the cordoning off of the city. As such, a revised performance object matrix has been suggested that limits building damage to be repairable and operational under a rare and very rare earthquake event. To achieve these performance targets, it is likely that engineers will have to employ better materials and technologies. The performance of shape memory alloys (SMAs) could be used as a substitute material to typical steel reinforcement in walls to increase the operational performance of these salient elements.

The residual displacements of RC walls with conventional steel were investigated in this paper. Using an extensive number of force-displacement hysteresis from experimental wall specimens, the residual displacements were calculated and presented as a function of the in-plane drift. It was shown that, on average, these conventional walls can typically sustain a drift level of approximately 1.5% prior to exceeding the permissible residual displacement limit of 0.005 rad. Using a limited dataset of RC walls detailed with SMAs in the boundary ends, it was shown that a slightly better performance (with regards to the residual displacement) could be achieved. For walls with SMA rebars, an average drift of approximately 2.0% can be attained prior to reaching this permissible limit imposed on the residual displacements. However, the dataset used for the RC-SMA walls is very limited and some of the walls were observed to perform poorly due to the light amount of steel that had been detailed in the web of the wall. Thus, more experimental research is needed in this area to confirm some of the results found here.

7 References

Aaleti, S., Brueggen, B. L., Johnson, B., French, C. E., & Sritharan, S. (2013). Cyclic Response of Reinforced Concrete Walls with Different Anchorage Details: Experimental Investigation. Journal of Structural Engineering, 139(7), 1181-1191. doi:10.1061/(ASCE)ST.1943-541X.0000732

Abdulridha, A., & Palermo, D. (2017). Behaviour and modelling of hybrid SMA-steel reinforced concrete slender shear wall. Engineering Structures, 147, 77-89. doi:10.1016/j.engstruct.2017.04.058

ACI. (2019). Building Code Requirements for Structural Concrete (ACI 318-19). Farmington Hills, MI: American Concrete Institute.

Almeida, J., Prodan, O., Rosso, A., & Beyer, K. (2017). Tests on Thin Reinforced Concrete Walls Subjected to In-Plane and Out-of-Plane Cyclic Loading. Earthquake Spectra, 33(1), 323-345. doi:10.1193/101915eqs154dp

Almeida, J. P. d., Steinmetz, M., Rigot, F., & de Cock, S. (2020). Shape-memory NiTi alloy rebars in flexural-controlled large-scale reinforced concrete walls: Experimental investigation on self-centring and damage limitation. Engineering Structures, 220, 110865. doi:10.1016/j.engstruct.2020.110865

ASCE. (2010). American society of civil engineers/structural engineering institute ASCE/SEI 7-10, Minimum design loads for buildings and other structures. Reston, Virginia. doi:10.1061/9780784412916

Brueggen, B. L., French, C. E., & Sritharan, S. (2017). T-Shaped RC Structural Walls Subjected to Multidirectional Loading: Test Results and Design Recommendations. Journal of Structural Engineering, 143(7), 04017040.

Buchanan, A., Bull, D., Dhakal, R., MacRae, G., Palermo, P., & Pampanin, S. (2011). Base Isolation and Damage-Resistant Technologies for Improved Seismic Performance of Buildings, Report to the Royal Commission for the Canterbury Earthquakes, New Zealand, August 2011. In.

CEN. (2004). Eurocode 8: Design of structures for earthquake resistance. Part 1: general rules, seismic actions and rules for buildings. In E. S. E. 1998-1:2004 (Ed.). In. Brussels, Belgium, 2004: Comité Européen de Normalisation.

Dashti, F., Dhakal, R. P., & Pampanin, S. (2020). Out-of-Plane Response of In-Plane-Loaded Ductile Structural Walls: State-of-the-Art and Classification of the Observed Mechanisms. Journal of Earthquake Engineering, 1-22. doi:10.1080/13632469.2020.1713928

Dazio, A., Beyer, K., & Bachmann, H. (2009). Quasi-static cyclic tests and plastic hinge analysis of RC structural walls. Engineering Structures, 31(7), 1556-1571. doi:10.1016/j.engstruct.2009.02.018

Deng, M., Liang, X., & Yang, K. (2008). Experimental study on seismic behavior of high performance concrete shear wall with new strategy of transverse confining stirrups. Paper presented at the Proceeding of the 14th World Conference on Earthquake Engineering, Xi'an University of Architecture & Technology, China.

Ghobarah, A. (2001). Performance-based design in earthquake engineering: state of development. Engineering Structures, 23(8), 878-884.

Goldsworthy, H. M. (2012). Lessons on building design from the 22 February 2011 Christchurch earthquake. Australian Journal of Structural Engineering, 13(2), 159. doi:10.7158/S11-136.2012.13.2

Graesser, E. J., & Cozzarelli, F. A. (1991). Shape-Memory Alloys as New Materials for Aseismic Isolation. Journal of Engineering Mechanics, 117(11), 2590-2608. doi:10.1061/(ASCE)0733-9399(1991)117:11(2590).

Hirosawa, M. (1975). Past experimental results on reinforced concrete shear walls and analysis on them. Kenchiku Kenkyu Shiryo, 6, 33-34.

Jani, J. M., Leary, M., Subic, A., & Gibson, M. A. (2014). A review of shape memory alloy research, applications and opportunities. Materials & Design (1980-2015), 56, 1078-1113.

Kam, W. Y., Pampanin, S., & Elwood, K. J. (2011). Seismic performance of RC buildings in the 22 February Christchurch (Lyttelton) earthquake. Bulletin of the New Zealand National Society for Earthquake Engineering, 44(4).

Kian, M. J. T., & Cruz-Noguez, C. (2018). Reinforced Concrete Shear Walls Detailed with Innovative Materials: Seismic Performance. Journal of Composites for Construction, 22(6), 04018052. doi:10.1061/(ASCE)CC.1943-5614.0000893

Krawinkler, H., & Miranda, E. (2004). Performance-based earthquake engineering. Earthquake engineering: from engineering seismology to performance-based engineering, 9, 1-9.

Lefas, I., D. , & Kotsovos, M. D. (1990). Strength and Deformation Characteristics of Reinforced Concrete Walls Under Load Reversals. ACI Structural Journal, 87(6). doi:10.14359/2994

Lowes, L. N., Lehman, D. E., Birely, A. C., Kuchma, D. A., Marley, K. P., & Hart, C. R. (2012). Earthquake response of slender planar concrete walls with modern detailing. Engineering Structures, 43, 31-47. doi:10.1016/j.engstruct.2012.04.040

Lu, X., Zhou, Y., Yang, J., Qian, J., Song, C., & Wang, Y. (2010). Shear Wall Database. Network for Earthquake Engineering Simulation (database).

Lu, Y., & Henry, R. S. (2021). Data Set for Cyclic Tests of Eleven Lightly Reinforced Concrete Walls. 147(3), 04720004. doi:10.1061/(ASCE)ST.1943-541X.0002942

McCormick, J., Aburano, H., Ikenaga, M., & Nakashima, M. (2008). Permissible residual deformation levels for building structures considering both safety and human elements. Paper presented at the Proceedings of the 14th world conference on earthquake engineering, Beijing, China.

Menegon, S. J., Wilson, C. J. N., Lam, N. T. K., & Gad, E. F. (2017). Experimental Testing of Reinforced Concrete Walls in Regions of Lower Seismicity. Bulletin of the New Zealand Society for Earthquake Engineering, 50(4).

Muir-Wood, R. (2015). The Christchurch earthquakes of 2010 and 2011. The Geneva risk reports. Risk and insurance research. Extreme events and insurance: 2011 Annus horribilis. Courbage C, Stahel WR, Geneva. In.

NRCC (2010). National Building Code of Canada, Associate Committee on the National Building Code, National Research Council of Canada, Ottawa, ON

NZ 3101. (2006). Standards Association NZ, NZ 3101: Part1:2006, "Concrete Structures Standard - The Design of Concrete Structures". In.

Perus, I., Biskinis, D., Fajfar, P., Fardis, M. N., Grammatikou, S., Krawinkler, H., & Lignos, D. (2014). The SERIES Database of RC elements. Paper presented at the 2nd European Conference on Earthquake Engineering and Seismology, Istanbul.

Rosso, A., Almeida, J. P., Constantin, R., Beyer, K., & Sritharan, S. (2014, 25-29 August, 2014). Influence of longitudinal reinforcement layouts on RC wall performance. Paper presented at the Second European Conference on Earthquake Engineering and Seismology, Istanbul.

Rosso, A., Jiménez-Roa, L. A., Almeida, J. P. D., & Beyer, K. (2020). Instability of Thin Concrete Walls with a Single Layer of Reinforcement under Cyclic Loading: Numerical Simulation and Improved Equivalent Boundary Element Model for Assessment. Journal of Earthquake Engineering, 1-32. doi:10.1080/13632469.2019.1691679

SEAOC. (1995). Vision 2000, Performance based seismic engineering of buildings, vols. I and II: Conceptual Framework. Sacramento (CA): Structural Engineers Association of California.

Sritharan, S., Beyer, K., Henry, R. S., Chai, Y. H., Kowalsky, M., & Bull, D. (2014). Understanding Poor Seismic Performance of Concrete Walls and Design Implications. Earthquake Spectra, 30(1), 307-334. doi:10.1193/021713EQS036M

Standards Australia. (2007). AS 1170.4-2007: Structural design actions, Part 4: Earthquake actions in Australia (Incorporating Amendments Nos 1 and 2).

Standards Australia. (2018). AS 3600-2018: Concrete Structures.

Su, R. K. L., & Wong, S. M. (2007). Seismic behaviour of slender reinforced concrete shear walls under high axial load ratio. Engineering Structures, 29(8), 1957-1965. doi:10.1016/j.engstruct.2006.10.020

Tasnimi, A. A. (2000). Strength and deformation of mid-rise shear walls under load reversal. Engineering Structures, 22(4), 311-322. doi:10.1016/S0141-0296(98)00110-2

Thomsen, J., & Wallace, J. (2004). Displacement-Based Design of Slender Reinforced Concrete Structural Walls—Experimental Verification. Journal of Structural Engineering, 130(4), 618-630. doi:10.1061/(ASCE)0733-9445(2004)130:4(618)

Tokunaga, R., & Nakachi, T. (2012). Experimental Study on Edge Confinement of Reinforced Concrete Core Walls. Paper presented at the Fifteenth World Conference on Earthquake Engineering, Lisbon.

Zhou, Y., Zhang, D., Huang, Z., & Li, D. (2014). Deformation Capacity and Performance-Based Seismic Design for Reinforced Concrete Shear Walls. Journal of Asian Architecture and Building Engineering, 13(1), 209-215. doi:10.3130/jaabe.13.209

8 Data Availability

The experimental dataset from this research paper, in conjunction with some other research conducted by the authors, can be downloaded from the publicly accessible platform Dataverse, DOI: 10.14428/DVN/A1FZT9. The structure of the data folders is described in the report 'Data_organization_Hoult_and_Almeida_2021.pdf', also available for download.

9 Appendix

Table A1 Experimental reinforced concrete wall specimens detailed with conventional steel; the full reference list and corresponding publications can be found on Dataverse (see Section 8)

Wall Specimen	Reference	t_w [mm]	L_w [mm]	h_s [mm]	L_v [mm]	ALR [%]	ρ_{lb} [%]	ρ_{lw} [%]
TW1	Almeida *et al.* (2017)	80	2700	2000	10000	4.3	2.63	0.15
TW4	Almeida *et al.* (2017)	80	2700	2000	10000	3.3	2.63	0.15
TW5	Almeida *et al.* (2017)	120	2700	2000	7350	4.8	0.50	0.50
WSH1	Dazio *et al.* (2009)	150	2000	4560	4560	5.1	1.32	0.30
WSH2	Dazio *et al.* (2009)	150	2000	4560	4560	5.7	1.32	0.30
WSH3	Dazio *et al.* (2009)	150	2000	4560	4560	5.8	1.54	0.54
WSH4	Dazio *et al.* (2009)	150	2000	4560	4560	5.7	1.54	0.54
WSH5	Dazio *et al.* (2009)	150	2000	4560	4560	12.8	0.67	0.27
WSH6	Dazio *et al.* (2009)	150	2000	4560	4560	10.8	1.54	0.54
HCPW_01	Deng *et al.* (2008)	100	1000	2100	2100	21.0	2.66	0.30
HCPW_02	Deng *et al.* (2008)	100	1000	2100	2100	21.0	2.66	0.30
HCPW_03	Deng *et al.* (2008)	100	1000	2100	2100	28.0	2.70	0.30
HCPW_04	Deng *et al.* (2008)	100	1000	2100	2100	28.0	2.30	0.15
Ho1	Hirosawa (1975)	160	850	1700	1700	10.0	0.85	0.30
Ho2	Hirosawa (1975)	160	850	1700	1700	10.0	0.85	0.30
Ho3	Hirosawa (1975)	160	850	1700	1700	10.0	0.85	0.30

Ho4	Hirosawa (1975)	160	850	1700	1700	10.0	0.85	0.30
SW31	Lefas and Kotsovos (1990)	65	650	1425	1425	0.0	3.00	1.50
SW32	Lefas and Kotsovos (1990)	65	650	1425	1425	0.0	3.00	1.50
SW33	Lefas and Kotsovos (1990)	65	650	1425	1425	0.0	3.00	1.50
PW1	Lowes *et al.* (2012)	152	3048	3658	8490	9.5	3.40	1.00
PW2	Lowes *et al.* (2012)	152	3048	3658	6065	13.0	3.40	1.00
PW3	Lowes *et al.* (2012)	152	3048	3658	6065	10.0	2.00	2.00
PW4	Lowes *et al.* (2012)	152	3048	3658	6065	12.0	3.40	1.00
C1	Lu and Henry (2021)	150	1400	2800	2800	3.5	0.53	0.53
C2	Lu and Henry (2021)	150	1400	2800	5600	3.5	0.53	0.53
C3	Lu and Henry (2021)	150	1400	2800	8400	3.5	0.53	0.53
C4	Lu and Henry (2021)	150	1400	2800	2800	0.0	0.53	0.53
C5	Lu and Henry (2021)	150	1400	2800	2800	6.6	0.53	0.53
C6	Lu and Henry (2021)	150	1400	2800	5600	3.5	0.53	0.53
M1	Lu and Henry (2021)	150	1400	2800	5600	3.5	1.00	0.47
M2	Lu and Henry (2021)	150	1400	2800	5600	3.5	1.44	0.47
M3	Lu and Henry (2021)	150	1400	2800	5600	3.5	0.72	0.47
M4	Lu and Henry (2021)	150	1400	2800	5600	3.5	1.28	0.47
M5	Lu and Henry (2021)	150	1400	2800	2800	3.5	1.00	0.47
S01	Menegon *et al.* (2017)	200	1200	2600	7800	5.8	3.67	3.67
W1	Su and Wong (2007)	80	400	1640	1640	25.0	1.96	1.96
W2	Su and Wong (2007)	80	400	1640	1640	50.0	1.96	1.96
W3	Su and Wong (2007)	80	400	1640	1640	50.0	1.96	1.96
SHW1	Tasnimi (2000)	50	500	1500	1500	0.0	2.26	0.28
SHW2	Tasnimi (2000)	50	500	1500	1500	0.0	2.26	0.28
SHW3	Tasnimi (2000)	50	500	1500	1500	0.0	2.26	0.28
SHW4	Tasnimi (2000)	50	500	1500	1500	0.0	2.26	0.28
RW1	Thomsen and Wallace (2004)	102	1219	3658	3658	10.0	3.00	0.33
RW2	Thomsen and Wallace (2004)	102	1219	3658	3658	10.0	3.00	0.33
H1	Tokunaga and Nakachi (2012)	90	430	1050	1050	40.0	3.25	3.25
H2	Tokunaga and Nakachi (2012)	90	430	1050	1050	40.0	3.25	3.25

H3	Tokunaga and Nakachi (2012)	90	430	1050	1050	20.0	3.25	3.25
No1	Tokunaga and Nakachi (2012)	90	430	1050	1050	20.0	3.25	3.25
No2	Tokunaga and Nakachi (2012)	90	430	1050	1050	40.0	3.25	3.25
No3	Tokunaga and Nakachi (2012)	90	430	1050	1050	20.0	3.25	3.25
No4	Tokunaga and Nakachi (2012)	90	430	1050	1050	40.0	3.25	3.25
No5	Tokunaga and Nakachi (2012)	90	430	1050	1050	20.0	3.25	3.25
No6	Tokunaga and Nakachi (2012)	90	430	1050	1050	40.0	3.25	3.25
No7	Tokunaga and Nakachi (2012)	90	430	1050	1050	20.0	3.25	3.25
No8	Tokunaga and Nakachi (2012)	90	430	1050	1050	40.0	3.25	3.25
SW1_0	Zhou *et al.* (2014)	180	900	2250	2250	20.0	0.75	0.84
SW1_1	Zhou *et al.* (2014)	125	1000	2000	2000	21.0	0.32	0.38
SW1_2	Zhou *et al.* (2014)	125	1000	2000	2000	43.0	0.32	0.38
SW1_3	Zhou *et al.* (2014)	125	1000	2000	2000	64.0	0.32	0.38
SW1_4	Zhou *et al.* (2014)	125	1000	2000	2000	86.0	0.32	0.38
SW2_0	Zhou *et al.* (2014)	180	900	2250	2250	0.0	0.75	0.84
SW2_1	Zhou *et al.* (2014)	125	1000	2000	2000	30.0	0.32	0.38
SW2_2	Zhou *et al.* (2014)	125	1000	2000	2000	30.0	0.32	0.38
SW2_3	Zhou *et al.* (2014)	125	1000	2000	2000	30.0	0.32	0.38
SW3_0	Zhou *et al.* (2014)	180	900	2250	2250	0.0	0.75	0.84
SW4_0	Zhou *et al.* (2014)	180	900	2250	2250	20.0	0.75	0.84
SW4_1	Zhou *et al.* (2014)	125	1000	2000	2000	30.0	0.24	0.38
SW4_2	Zhou *et al.* (2014)	125	1000	2000	2000	30.0	0.32	0.38
SW4_3	Zhou *et al.* (2014)	125	1000	2000	2000	30.0	0.32	0.38
SW5_1	Zhou *et al.* (2014)	125	1000	2000	2000	30.0	0.32	0.38
SW5_2	Zhou *et al.* (2014)	125	1000	2000	2000	30.0	0.32	0.38
SW5_3	Zhou *et al.* (2014)	125	1000	2000	2000	30.0	0.32	0.38
SW6_1	Zhou *et al.* (2014)	125	1000	2000	2000	30.0	0.32	0.38
SW6_2	Zhou *et al.* (2014)	125	1000	2000	2000	30.0	0.32	0.38
SW6_3	Zhou *et al.* (2014)	125	1000	2000	2000	30.0	0.32	0.38

Table A2 Experimental reinforced concrete wall specimens detailed with shape memory alloys; the full reference list and corresponding publications can be found on Dataverse (see Section 8)

Wall Specimen	Reference	t_w [mm]	L_w [mm]	h_s [mm]	L_v [mm]	ALR [%]	ρ_{lb} [%]	ρ_{lw} [%]
W2-NR	Abdulridha and Palermo (2017)	150	1000	2200	2400	0.0	1.69	0.67
SMA-SFRC	Kian and Cruz-Noguez (2018)	150	1000	2000	2005	0.0	1.69	0.67
RC-SMA	Almeida *et al.* (2020)	100	1200	2000	4320	3.0	1.80	0.56